Research Article
Experimental and Translational Hepatology

JOURNAL OF HEPATOLOGY

STARD1 promotes NASH-driven HCC by sustaining the generation of bile acids through the alternative mitochondrial pathway

Laura Conde de la Rosa[1,2,3], Carmen Garcia-Ruiz[1,2,3,4,*], Carmen Vallejo[1,2,3], Anna Baulies[1,2,3], Susana Nuñez[1,2,3], Maria J. Monte[3,5], Jose J.G. Marin[3,5], Lucia Baila-Rueda[6,7], Ana Cenarro[6,7], Fernando Civeira[6,7], Josep Fuster[8], Juan C. Garcia-Valdecasas[8], Joana Ferrer[8], Michael Karin[9], Vicent Ribas[1,2,3,*], Jose C. Fernandez-Checa[1,2,3,4,*]

[1]*Department of Cell Death and Proliferation, Institute of Biomedical Research of Barcelona (IIBB), CSIC, Barcelona, Spain;* [2]*Liver Unit, Hospital Clinic I Provincial de Barcelona, Instituto de Investigaciones Biomédicas August Pi i Sunyer (IDIBAPS), Barcelona, Spain;* [3]*Center for the Study of Liver and Gastrointestinal Diseases (CIBERehd), Carlos III National Institute of Health, Madrid, Spain;* [4]*Center for ALPD, Keck School of Medicine, University of Southern California, Los Angeles, CA, USA;* [5]*Experimental Hepatology and Drug Targeting (HEVEFARM), Institute of Biomedical Research of Salamanca (IBSAL), University of Salamanca, Salamanca, Spain;* [6]*Instituto Investigación Sanitaria Aragón, Hospital Universitario Miguel Servet, Zaragoza, Spain;* [7]*CIBERCV, Madrid, Spain;* [8]*HepatoBilioPancreatic Surgery and Liver and Pancreatic Transplantation Unit, Department of Surgery, ICMDiM, Hospital Clinic, University of Barcelona, Barcelona, Spain;* [9]*Laboratory of Gene Regulation and Signal Transduction, Department of Pharmacology, School of Medicine, University of California San Diego, La Jolla, CA, USA*

Background & Aims: Besides their physiological role in bile formation and fat digestion, bile acids (BAs) synthesised from cholesterol in hepatocytes act as signalling molecules that modulate hepatocellular carcinoma (HCC). Trafficking of cholesterol to mitochondria through steroidogenic acute regulatory protein 1 (STARD1) is the rate-limiting step in the alternative pathway of BA generation, the physiological relevance of which is not well understood. Moreover, the specific contribution of the STARD1-dependent BA synthesis pathway to HCC has not been previously explored.

Methods: STARD1 expression was analyzed in a cohort of human non-alcoholic steatohepatitis (NASH)-derived HCC specimens. Experimental NASH-driven HCC models included MUP-uPA mice fed a high-fat high-cholesterol (HFHC) diet and diethylnitrosamine (DEN) treatment in wild-type (WT) mice fed a HFHC diet. Molecular species of BAs and oxysterols were analyzed by mass spectrometry. Effects of NASH-derived BA profiles were investigated in tumour-initiated stem-like cells (TICs) and primary mouse hepatocytes (PMHs).

Results: Patients with NASH-associated HCC exhibited increased hepatic expression of STARD1 and an enhanced BA pool. Using NASH-driven HCC models, STARD1 overexpression in WT mice increased liver tumour multiplicity, whereas hepatocyte-specific STARD1 deletion (*Stard1*$^{\Delta Hep}$) in WT or MUP-uPA mice reduced tumour burden. These findings mirrored the levels of unconjugated primary BAs, β-muricholic acid and cholic acid, and their tauroconjugates in STARD1-overexpressing and *Stard1*$^{\Delta Hep}$ mice. Incubation of TICs or PMHs with a mix of BAs mimicking this profile stimulated expression of genes involved in pluripotency, stemness and inflammation.

Conclusions: The study reveals a previously unrecognised role of STARD1 in HCC pathogenesis, wherein it promotes the synthesis of primary BAs through the mitochondrial pathway, the products of which act in TICs to stimulate self-renewal, stemness and inflammation.

Lay summary: Effective therapy for hepatocellular carcinoma (HCC) is limited because of our incomplete understanding of its pathogenesis. The contribution of the alternative pathway of bile acid (BA) synthesis to HCC development is unknown. We uncover a key role for steroidogenic acute regulatory protein 1 (STARD1) in non-alcoholic steatohepatitis-driven HCC, wherein it stimulates the generation of BAs in the mitochondrial acidic pathway, the products of which stimulate hepatocyte pluripotency and self-renewal, as well as inflammation.

Introduction

Hepatocellular carcinoma (HCC) is the most common type of liver cancer and the end stage of chronic liver disease caused by different aetiologies, including non-alcoholic steatohepatitis (NASH). The incidence of NASH-driven HCC is expected to increase worldwide because of its association with the obesity and type 2 diabetes mellitus epidemic. Overweight (body mass index >25) and obesity are known risk factors for cancer development, especially HCC.[1,2] HCC has a poor prognosis with frequent recurrence and metastasis.[2,3] Although important improvements in the management of HCC have been made over the past 2 or 3 decades, effective treatment options, such as local ablative therapies, resection or transplantation, are mainly limited to early disease stages.[4,5] Unfortunately, the therapeutic armamentarium for HCC is limited, ineffective and subject to secondary or acquired chemoresistance by currently poorly understood mechanisms.[6] Hence, there is an urgent need to understand HCC pathogenesis and identify new therapeutic targets.

Keywords: Cholesterol; Mitochondria; Bile acids; Hepatocellular carcinoma; Oxysterols; STARD1.
Received 19 June 2020; received in revised form 10 January 2021; accepted 13 January 2021; available online 27 January 2021
* Corresponding authors. Address: Department of Cell Death and Proliferation, Institute of Biomedical Research of Barcelona (IIBB), CSIC, Barcelona, Spain.
E-mail addresses: vicente.ribas@iibb.csic.es (V. Ribas), cgrbam@iibb.csic.es (C. Garcia-Ruiz), checa229@yahoo.com (J.C. Fernandez-Checa).
https://doi.org/10.1016/j.jhep.2021.01.028

Diet-induced NASH and chronic endoplasmic reticulum (ER) stress have been shown to lead to HCC development.[7–9] Cancer cells are under anabolic pressure for the synthesis of membrane lipids to sustain dysregulated cell proliferation, and increased cholesterol and fatty acid synthesis support HCC growth.[10] Consistent with a key structural and functional role of cholesterol in membrane bilayers, recent reports indicated that dietary or *de novo*-synthesised cholesterol fosters HCC development, in part, through the generation of bile acids (BAs).[11–14] BAs are synthesised in hepatocytes from cholesterol predominantly through the classical (neutral) pathway, which is regulated by the rate-limiting enzyme 7-α-hydroxylase (encoded by *CYP7A1*). In addition, sterol 12α-hydroxylation by 12α-hydroxylase (encoded by *CYP8B1*) is specifically required for cholic acid (CA) synthesis. In addition to their key role in fat digestion and vitamin metabolism, BAs are critical signalling molecules that regulate gene expression by targeting nuclear (*e.g.* farnesoid X receptor; FXR) and membrane (*e.g.* Takeda G-protein-coupled receptor 5; TGR5) receptors and have been linked to NASH progression and HCC promotion.[14–16] Indeed, the severity of human NASH has been associated with specific changes in plasma levels of BAs, while mouse models (*e.g.* *FXR*$^{-/-}$, *BSEP*$^{-/-}$ or *MDR2*$^{-/-}$ mice) with an increase in total circulating BAs exhibit spontaneous formation of HCC.[16–19]

The mitochondrial pool of cholesterol is minor compared with its plasma membrane content and modulates vital mitochondrial functions, such as oxidative phosphorylation, mitochondrial apoptosis, chemotherapy resistance or susceptibility to tumour necrosis factor (TNF)/Fas-mediated NASH progression.[20–26] The mitochondrial cholesterol level is regulated by specific carriers, most notably steroidogenic acute regulatory protein 1 (STARD1), which mediates the trafficking of cholesterol to the mitochondrial inner membrane for metabolism.[27–29] In the liver, mitochondrial cholesterol is metabolised by 27-hydroxylase (encoded by *CYP27A1*) to 27-hydroxycholesterol followed by 25-hydroxycholesterol 7-α-hydroxylase (encoded by *CYP7B1*), which then feeds the alternative mitochondrial pathway of BA synthesis, leading mainly to chenodeoxycholic acid (CDCA) generation.[15,30,31] In mouse liver, CDCA is metabolised to α-muricholic acid (αMCA) and its 7β-epimer β-muricholic acid (βMCA).[32] The mitochondrial acidic pathway of BA synthesis is considered to contribute to a minor extent to the total BA pool and its physiological relevance is not well understood.

Patients with NASH exhibit elevated free cholesterol[33,34] and enhanced STARD1 expression.[33] Given that the contribution of the alternative pathway of BA synthesis to HCC has not been previously addressed, this study investigated the role of STARD1 in NASH-driven HCC. The results revealed a previously unrecognised role for STARD1 in HCC by stimulating the generation of BAs from cholesterol via the alternative pathway, the products of which act in tumour-initiating stem-like cells (TICs) and hepatocytes to stimulate expression of genes involved in pluripotency, stemness and inflammation.

Materials and methods

Human NASH-derived HCC cohort

Human liver samples were obtained from donors and recipients undergoing liver transplantation at the Liver Transplantation Unit of the Hospital Clinic, Barcelona (Table S1). During the donor sample procurement, an intraoperative assessment of the liver was systematically carried out to rule out fibrosis, cirrhosis, steatosis and other abnormalities before transplantation. A biopsy of the resected liver from the recipient was performed immediately after the hepatectomy and samples were fixed in formalin for histological evaluation or quickly snap-frozen. Samples from controls (donors) with signs of steatosis, fibrosis or inflammation were discarded. Recipients with NASH-derived HCC eligible for liver transplantation were compiled based on the Milan Criteria and were stratified by the Barcelona Clinic Liver Cancer score (single tumour ≤5 cm or 2–3 tumours ≤3 cm each).[35] Samples from individuals with viral hepatitis, alcoholic steatohepatitis or cryptogenic cirrhosis were excluded. NASH-derived HCC samples were processed for RNA isolation, western blotting and staining with GST-PFO and filipin. The protocol (HCB/2012/8011) was approved by the HCB/UB Ethics Committee of the Hospital Clinic of Barcelona, Spain.

Stard1$^{\Delta Hep}$ and MUP-uPA-*Stard1*$^{\Delta Hep}$ mice

Liver-specific Stard1-knockout (*Stard1*$^{\Delta Hep}$) mice were created by crossing *Stard1*$^{f/f}$ mice, which were generated by the Cre-lox technology, with Alb-Cre mice, and have been recently characterised elsewhere.[36] *Stard1*$^{\Delta Hep}$ and *Stard1*$^{f/f}$ littermates were used in the study. MUP-uPA transgenic mice were generated and have been previously characterised.[37] MUP-uPA transgenic animals were crossed with *Stard1*$^{\Delta Hep}$ mice and backcrossed with *Stard1*$^{f/f}$ to select homozygous *Stard1*$^{f/f}$–MUP-uPA tg positives with or without Alb-Cre expression (MUP-uPA-*Stard1*$^{f/f}$ and MUP-uPA-*Stard1*$^{\Delta Hep}$), which were used in the study.

NASH-driven HCC development and treatment

For the induction of HCC, C57Bl/6j mice were injected i.p. with a single dose of diethylnitrosamine (DEN; 25 mg/kg) on postnatal day 14; 4 weeks later, the mice were introduced to different diets (Table S2). Animals were fed either a high-fat diet (HFD, containing 60% calories from fat) or a high fat-high cholesterol (HFHC, containing 60% calories from fat and added 0.5% cholesterol) diet for up to 32 weeks. Additionally, a regular diet with added cholesterol was custom-made (Teklad diet 2014 with 2% cholesterol; HC diet). In some cases, DEN-treated mice were fed a HFHC diet with added ezetimibe (EZE) (100 mg Ezetrol/kg of diet, equivalent to 10 mg/kg/day) and fed for 24 weeks. To determine the effect of EZE treatment on survival, DEN-treated mice were fed a HFHC diet for 52 weeks. At the time of sacrifice, animals were anaesthetised and exsanguinated; macroscopic tumours were counted and the liver was harvested and processed for subsequent analysis.

For the induction of heterotopic tumours induced by TICs, 8-week-old athymic nude immunodeficient mice (Charles River) were subcutaneously injected with 1×10^6 TICs in 100 μL at 1:1 PBS Matrigel high concentration (Corning #354248) either stably overexpressing Stard1 or green fluorescent protein (GFP) in the right or left flanks, respectively; tumours were allowed to grow for 3 weeks.

All procedures involving animals and their care were approved by the Ethics Committee of the University of Barcelona following national and European guidelines for the maintenance and husbandry of research animals.

TIC isolation and treatment

TICs (CD133$^+$/CD49f$^+$) were isolated from murine HCC, as described previously.[38] Briefly, resected HCC tissues were immediately dissected into small pieces and digested with collagenase. Suspended liver cells were stained with PE-anti-

CD133, APC-anti-CD49f and FITC-anti-CD45 antibodies (BD Biosciences) followed by fluorescence-activated cell sorting analysis, as described previously.[39] TICs and primary mouse hepatocytes (PMHs) were treated with the specified concentrations of BAs: cholic acid (CA; Sigma, C1129), βMCA (Sigma, SML2372) or taurocholic acid (TCA; Sigma, T4009) for 24 or 48 h and analysed for expression of pluripotency, stemness and inflammatory genes by quantitative (q)PCR.

Quantification and statistical analysis

All data are presented as mean ± SEM. In each experiment, N defines the sample size. The Student's *t* test was used to define differences between 2 groups. To define differences between more than 2 groups, 1-way analysis of variance (ANOVA) was used with a Bonferroni multiple comparison post-test, or Kruskal–Wallis non-parametric test for data displaying a non-Gaussian distribution. The criterion for significance was set at $p < 0.05$. Statistical analyses were performed using GraphPad Prism version 5. Given the variability of the *in vivo* studies, 6–12 mice were included per group to ensure statistical power.

Results

Patients with NASH-driven HCC exhibit increased expression of STARD1 and a high BA burden

Although the basal expression of STARD1 in the liver is low, STARD1 is upregulated in patients with NASH but not in subjects with steatosis alone.[33] However, the role of STARD1 in NASH-driven HCC has not been previously explored. The current study examined the expression of STARD1 in a cohort of patients with NASH-derived HCC (Table S1). Histology analyses revealed alterations in the parenchymal architecture of human HCC samples (Fig. S1A), exhibiting fat infiltration, increased liver triglycerides (TG) and fibrosis (Fig. S1B,C), reflected by Sirius Red staining and increased expression of fibrogenic genes *ACTA2* and *COL1A1* (Fig. S1D). Liver samples from patients with NASH-driven HCC exhibited increased levels of *STAR* gene transcript and STARD1 protein, compared with samples from control subjects (Fig. 1A). Moreover, liver sections from patients with HCC displayed increased immunohistochemical STARD1 staining (Fig. 1B). *STARD1* was expressed predominantly in hepatocytes, as indicated by the colocalisation of STARD1 with asialoglycoprotein receptor 1 and, to a minor extent, with Kupffer cells and hepatic stellate cells labelled with F4/80 and alpha smooth muscle actin (α-SMA), respectively (Fig. S2). Higher hepatic free cholesterol levels were observed by staining liver sections with GST-perfringolysin (GST-PFO) (Fig. 1C), which detects free cholesterol in membranes,[40] as well as by filipin staining and HPLC analysis (Fig. S1E,F). GST-PFO staining of liver sections from patients with NASH-driven HCC colocalised with cytochrome c immunofluorescence (Fig. 1D), indicating the presence of free cholesterol in mitochondria in human HCC, consistent with findings in experimental HCC.[22,26] Furthermore, human HCC

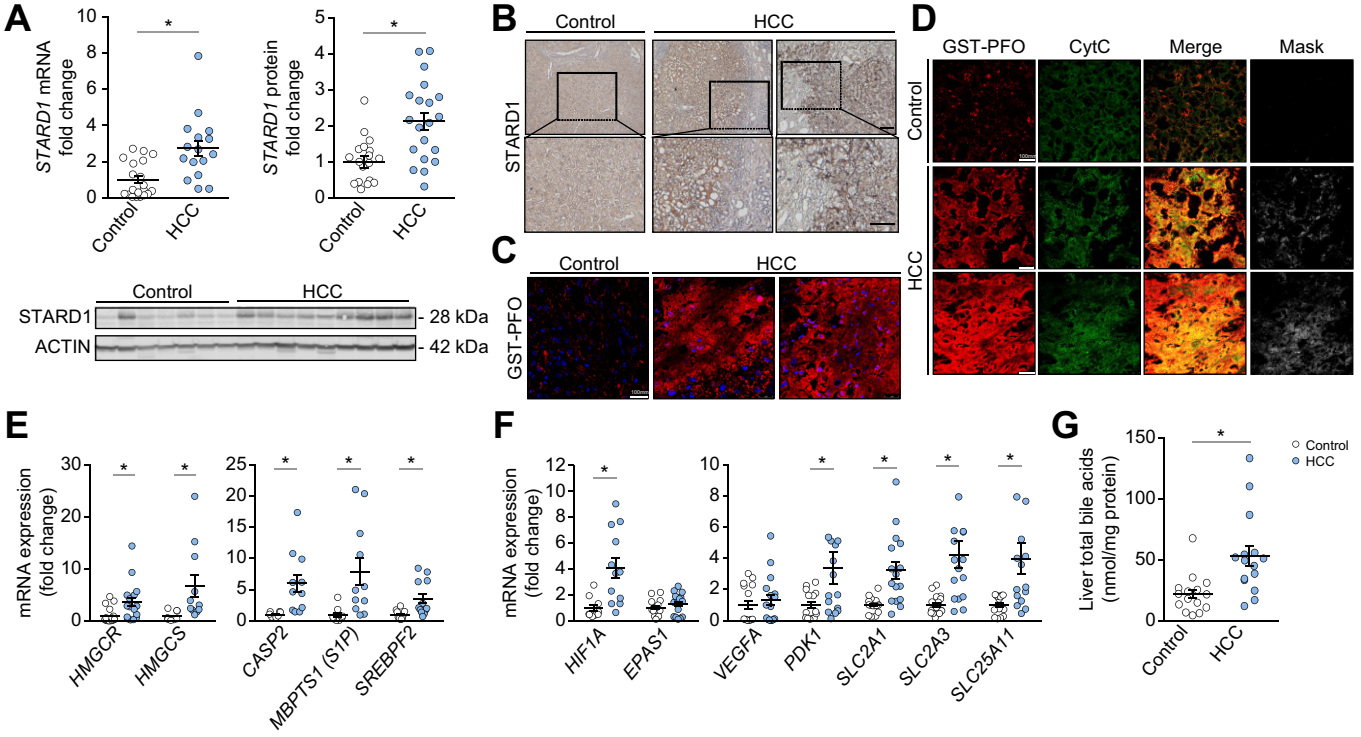

Fig. 1. Increased STARD1 expressed in human NASH-driven HCC. (A) Expression of *STAR* gene mRNA by qPCR and STARD1 protein in liver tissue from control donors and NASH-driven HCC (n = 15 controls, n = 15–20 patients with HCC). (B) Representative immunohistochemical expression of STARD1 from control and liver samples from patients with NASH-HCC. (C) Staining of liver sections from control and HCC samples with GST-PFO (red) to detect free cholesterol. Nuclei were stained with DAPI. (D) Immunostaining of liver sections from control and HCC samples with GST-PFO and Cyt C, showing their colocalisation as merge and mask. Scale bar: 75 μm. (E) Transcript quantification by qPCR of genes controlling cholesterol biosynthesis, ER stress-driven activation of *SREBP2*. (F) mRNA levels of *HIF1A* and HIF2A (*EPAS1*) and HIF-1α regulated genes. n = 13–18 controls, n = 13–20 patients with HCC. (G) Hepatic levels of total BAs in samples from controls and patients with HCC (n = 15 in both groups). All values are mean ± SEM. *$p < 0.05$ on Student's *t* test. Magnification bar in histology images: 100 μm. BA, bile acid; Cyt C cytochrome c; ER, endoplasmic reticulum; GST-PFO, GST-perfringolysin; HCC, hepatocellular carcinoma; NASH, non-alcoholic steatohepatitis; qPCR, quantitative PCR; STARD1, steroidogenic acute regulatory protein 1.

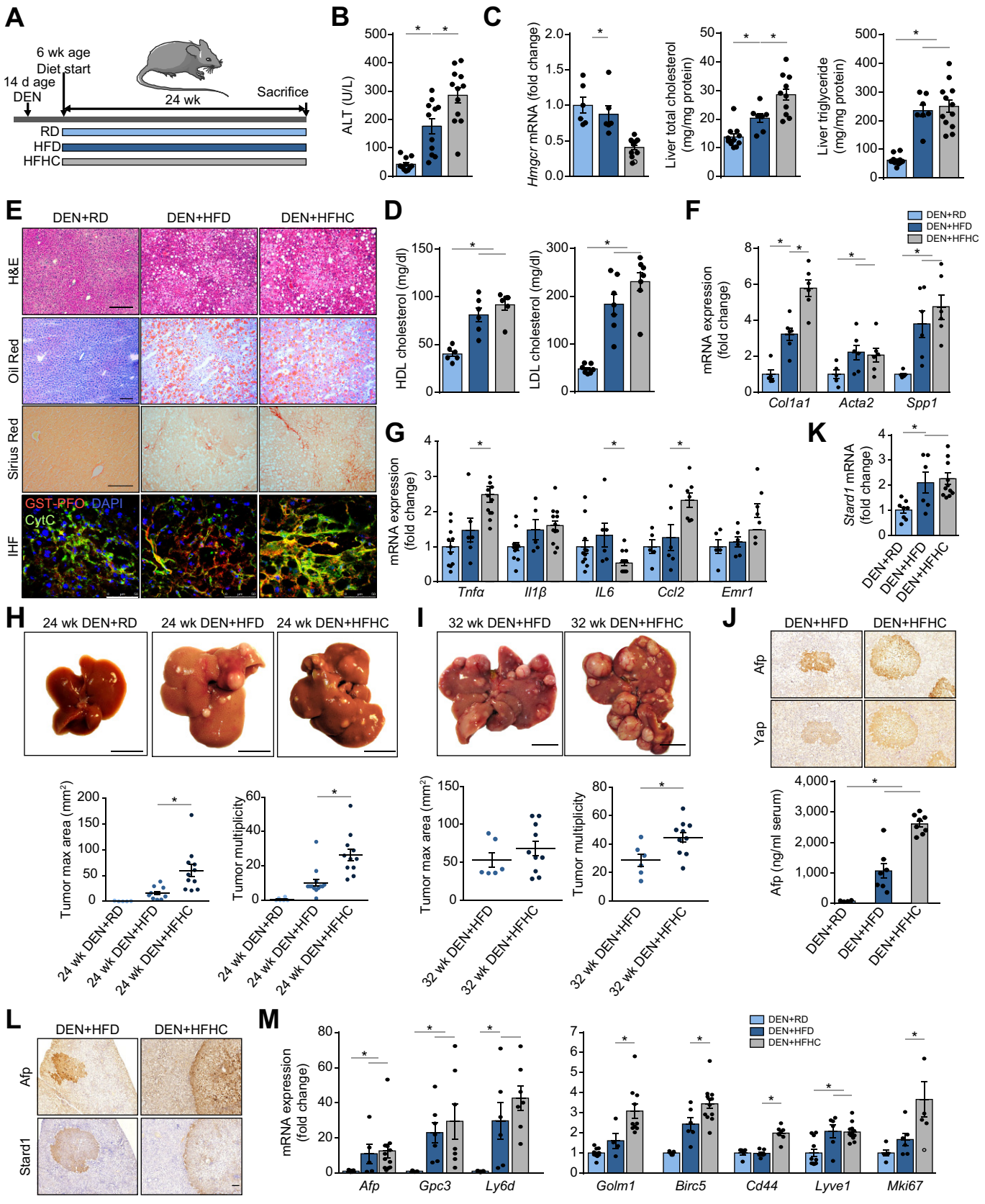

Fig. 2. HFHC feeding promotes NASH-driven HCC development in DEN-treated wild-type mice. (A) Schematic illustration of the experimental design, with induction of tumourigenesis in liver of mice with DEN at 14 days of age, feeding with RD, HFD, or HFHC diet for 24 weeks; n per group = 11 (RD), 12 (HFD and HFHC). (B) Serum ALT levels of mice after the corresponding treatments. (C) Liver *Hmgcr* transcript, total cholesterol and triglyceride liver composition; n = 6 per

samples exhibited increased expression of *HMGCS*, *HMGCR* and *SREBP2*, the master transcription factor for cholesterol homeostasis (Fig. 1E). Although SREBP2 is negatively regulated by cholesterol, the study addressed whether the activation of SREBP2 in association with increased cholesterol was linked to a refractory feedback loop triggered by the TNFR1-Caspase-2-S1P-SREBP2 axis.[41] Human HCC samples exhibited increased expression of *CASP-2* and *MBPTS1* (S1P) compared with control subjects (Fig. 1E). Moreover, samples from human HCC displayed increased expression of HIF1A and target genes, such as *PDK1, SLC2A1* (Glut 1), *SLC2A3* (Glut 3) and *SLC25A11* (2-OGC) (Fig. 1F), which have been shown to regulate mitochondrial GSH homeostasis in HCC.[38]

The study next examined the levels of the hepatic BA pool in patients with HCC. Compared with control subjects, human HCC samples revealed a 2-fold increase in total hepatic BA levels (Fig. 1G) that paralleled the increased expression of *CYP7A1, CYP8B1, CYP27A1* and *CYP7B1*, as well as *CYP7A1* and *CYP27A1* (Fig. S1G,H), suggesting the activation of the classical (neutral) and alternative (acidic) pathways of BA synthesis.

Cholesterol promotes NASH-driven HCC and induces STARD1 expression in mice

Next, the study addressed the specific contribution of the alternative mitochondrial pathway of BA generation to HCC. First, the tumour promoter role of cholesterol in HCC was validated because, despite accumulating evidence linking cholesterol with HCC development,[11–13] there have been studies showing a tumour-suppressor effect of cholesterol in HCC.[42–46] Given that a HFD alone does not induce NASH and DEN plus HFD feeding does not completely model NASH-driven HCC,[9] a dietary NASH-driven HCC approach was established by feeding DEN-pretreated mice with a HFD diet supplemented with cholesterol (HFHC) (Fig. 2A), because this diet has been shown to induce NASH.[47,48] Compared with mice fed DEN+HFD alone, DEN+HFHC-fed mice exhibited higher serum alanine aminotransferase (ALT) levels (Fig. 2B), enhanced liver cholesterol content and decreased *Hmgcr* expression (Fig. 2C). Serum HDL or LDL levels were independent on whether DEN-treated mice were fed a HFD or HFHC diet (Fig. 2D). Moreover, the degree of macrovesicular steatosis detected by Oil-Red staining and TG levels was similar between DEN+HFD and DEN+HFHC-fed mice (Fig. 2C,E), although fibrosis was more severe in DEN+HFHC-fed mice compared with DEN+HFD-fed mice (Fig. 2E,F). In addition, GST-PFO staining of liver sections of DEN+HFHC-fed mice revealed increased free cholesterol levels, which colocalised with cytochrome c (Fig. 2E). Furthermore, DEN+HFHC feeding increased liver inflammation, revealed by the enhanced expression of *Tnfa* and *Ccl2* (Fig. 2G). Of significance, whereas DEN+HFD feeding for 24 weeks had a modest impact on tumour burden relative to DEN alone, DEN+HFHC feeding resulted in a larger increase in tumour number and maximal area (Fig. 2H), which increased even further after 32 weeks of HFHC feeding (Fig. 2I). Tumour burden increased the levels of Afp in serum, especially in the DEN+HFHC group and these tumours displayed higher expression of Afp and Yap, 2 *bona fide* HCC markers (Fig. 2J). Moreover, DEN+HFHC feeding increased liver expression of Stard1 (Fig. 2K), which was preferentially expressed in HCC tumours (Fig. 2L). Furthermore, DEN+HFHC-fed mice exhibited increased expression of markers involved in tumourigenesis (*Gpc3*, *Ly6d*, and *Golm1*), cell adhesion and interactions (*Birc5*, *Cd44*, and *Lyve1*) and cellular proliferation (*Mki67*) with respect to DEN+HFD-fed mice (Fig. 2M).

Ezetimibe treatment attenuates DEN+HFHC-driven HCC

To further determine the role of cholesterol in NASH-driven HCC, the effect of EZE, which prevents the intestinal absorption of cholesterol, was tested. Although its role in human NASH is not well established,[49] its impact was examined in DEN+HFHC-driven HCC (Fig. S3A). EZE treatment decreased hepatic cholesterol accumulation in DEN+HFHC mice (Fig. S3B). The ability of EZE to decrease liver cholesterol resulted from its ability to block absorption of dietary cholesterol rather than affecting *de novo* cholesterol synthesis, consistent with the decreased expression of *Hmgcr and Hmgcs1* following HFHC feeding, indicating that dietary cholesterol exerts expected feedback inhibition on the *de novo* synthesis of cholesterol (Fig. S3C). Interestingly, the presence of EZE reversed the downregulation of *Hmgcr* and *Hmgcs1* in HFHC mice (Fig. S3C). In line with this outcome, treatment of HFHC mice with atorvastatin resulted in a modest effect in decreasing liver cholesterol (Fig. S4), in agreement with the lower expression of *Hmgcr* by dietary cholesterol. Of note, EZE did not change the expression of Stard1 in DEN+HFHC mice (Fig. S3C). Moreover, EZE ameliorated liver fibrosis in DEN+HFHC mice, as seen by Sirius Red staining and the decreased expression of fibrosis genes (Fig. S3D,E). Consistent with findings in $Pten^{\Delta Hep}$ mice fed a HFD,[50] the number of tumours in DEN+HFHC mice significantly decreased upon EZE administration (Fig. S3F), which paralleled the attenuation of serum Afp levels (Fig. S3G), the expression of markers of tumourigenesis, cell adhesion/migration and hepatic proliferation (Fig. S3H), and the decrease in the levels of Gp73 and cytokeratin 19 (Fig. S3I). More importantly, whereas the median survival of DEN+HFHC mice was 7 months, EZE treatment significantly increased the survival rate, with 50% of mice surviving 12 months post DEN+HFHC feeding (Fig. S3J).

group. (D) HDL or LDL levels in serum from DEN+HFD or DEN+HFHC mice; n = 6 per group. (E) Representative histological staining for haematoxylin and eosin (H&E), neutral lipid (Oil Red O) and collagen fibers (Sirius red) of liver sections. Immunohistofluorescence of liver sections stained for free cholesterol with GST-PFO probe (red), mitochondria with anti-cytochrome c (green) and nuclei with DAPI (blue). Scale bar: 100 μm. (F) mRNA levels of fibrogenesis-associated genes (*Col1a1*, *Acta2* and *Spp1*). All values were corrected by a housekeeping gene (*Actb*) and relative to values from the animals on a DEN-RD diet; n = 6–10 per group. (G) mRNA levels of inflammation genes (*Tnfa*, *Il1b*, *Il6*, *Ccl2* and *Emr1*). (H) Representative macroscopic images and quantification of tumour multiplicity and maximal area from DEN-treated mice fed a HFHC diet for 24 weeks. RD, n = 6; HFD, n = 10; HFHC, n = 11. (I) As in (H) except that DEN-treated mice were fed a HFHC diet for 32 weeks. HFD, n = 6; HFHC, n = 10. (J) Immunohistochemical expression of Afp and Yap of consecutive liver sections from DEN-treated mice fed either HFD or HFHC diet for 24 weeks. (K) mRNA levels of Stard1 of whole-liver tissue from DEN-treated mice fed RD or HFHC diet. n = 6–10 per group. (L) Immunohistochemistry of consecutive sections (T, tumour) stained for Afp or Star. Scale bar: 500 μm. (M) mRNA levels of tumour markers and inflammatory genes of whole-liver tissue from DEN-treated mice fed RD, HFD or HFHC; n = 6–10 per group. All values are mean ± SEM; *p <0.05 on a 12-way ANOVA test or Student's t test. ALT, aminotransferase; DEN, diethylnitrosamine; HCC, hepatocellular carcinoma; HFD, high-fat diet; HFHC, high fat, high cholesterol; GST-PFO, GST-perfringolysin; NASH, non-alcoholic steatohepatitis; RD, regular diet; Stard1, steroidogenic acute regulatory protein 1.

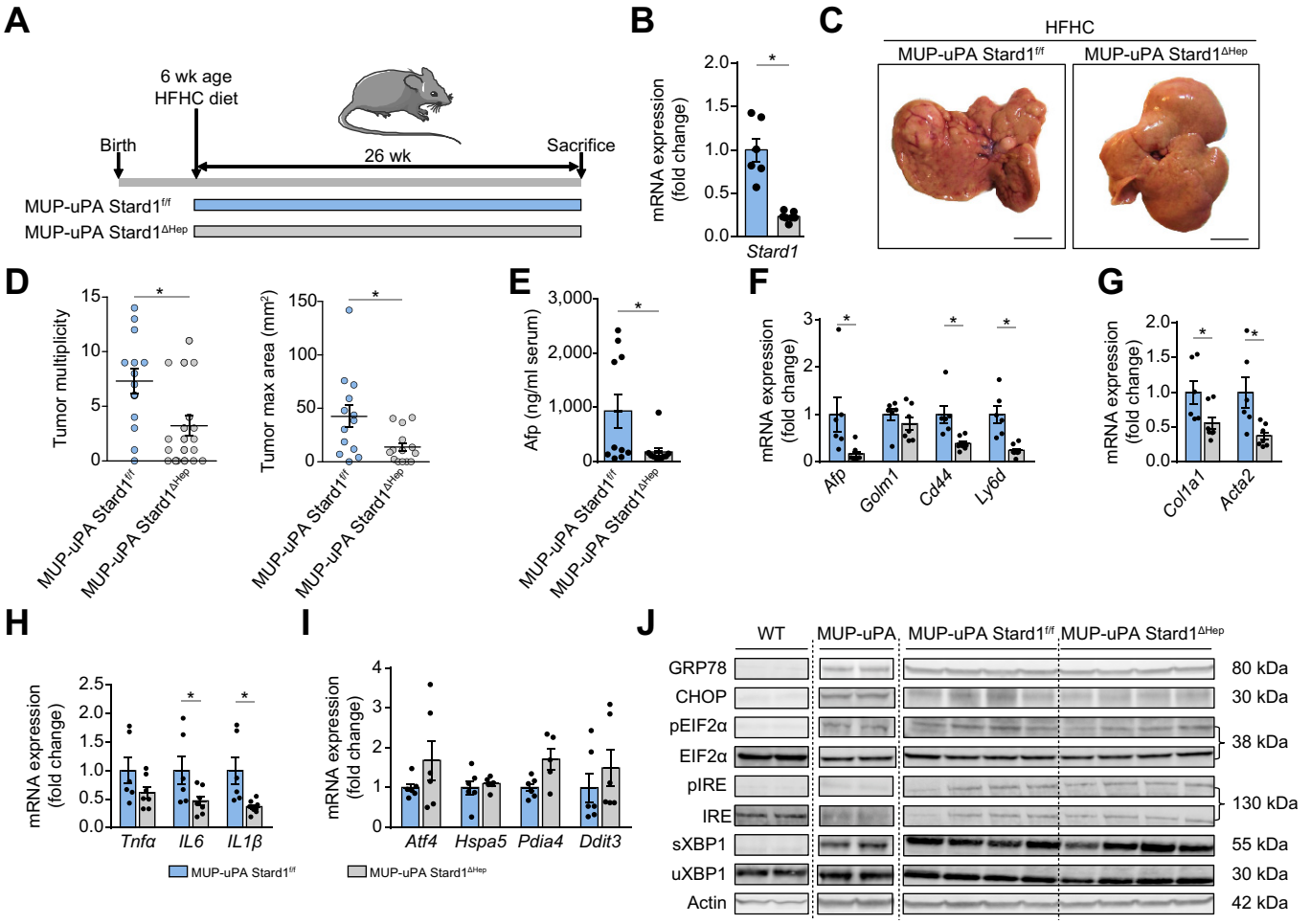

Fig. 3. Hepatocyte Stard1 deletion in MUP-uPA mice attenuates NASH-driven HCC in mice. (A) Feeding of MUP-uPA-*Stard1*$^{f/f}$ and MUP-uPA-*Stard1*$^{\Delta Hep}$ mice with HFHC diet for 26 weeks. (B) mRNA levels of Stard1 in MUP-uPA-*Stard1*$^{f/f}$ (n = 6) and MUP-uPA-*Stard1*$^{\Delta Hep}$ mice (n = 7). (C,D) Macroscopic images of livers from MUP-uPA-*Stard1*$^{f/f}$ (n = 13) and MUP-uPA-*Stard1*$^{\Delta Hep}$ mice (n = 14) fed a HFHC diet for 26 weeks, with quantification of tumour multiplicity and maximal area. (E) Serum Afp levels of MUP-uPA-*Stard1*$^{f/f}$ (n = 10) and MUP-uPA-*Stard1*$^{\Delta Hep}$ mice (n = 10) fed a HFHC diet. (F–H) mRNA levels of tumour markers, fibrosis and inflammation genes of whole-liver tissue from MUP-uPA-*Stard1*$^{f/f}$ (n = 6) and MUP-uPA-*Stard1*$^{\Delta Hep}$ mice (n = 7) fed a HFHC diet. (I) mRNA levels of ER stress markers of whole-liver tissue from MUP-uPA-*Stard1*$^{f/f}$ (n = 6) and MUP-uPA-*Stard1*$^{\Delta Hep}$ mice (n = 7) fed a HFHC diet. (J) Western blot of ER stress markers as in (H). All values are mean ± SEM. *p <0.05 with respect to MUP-uPA-*Stard1*$^{f/f}$ or *Stard1*$^{f/f}$ mice on a Student's t test. ER endoplasmic reticulum; HCC, hepatocellular carcinoma; HFHC, high fat, high cholesterol; NASH, non-alcoholic steatohepatitis; Stard1, steroidogenic acute regulatory protein 1.

Overall, these findings indicate that dietary cholesterol promotes NASH-driven HCC development.

STARD1 deletion in hepatocytes attenuates NASH-driven HCC

To address the role of STARD1 in NASH-driven HCC, Stard1$^{\Delta Hep}$ mice were generated[36] and their susceptibility to NASH-driven HCC was examined using 2 different approaches. First, STARD1 was deleted in hepatocytes in MUP-uPA mice, a model characterised by endogenous chronic ER stress because of the expression of urokinase plasminogen activator (uPA) and which develop HCC via the synergism between ER stress and overfeeding.[8,9] MUP-uPA mice were crossed with *Stard1*$^{\Delta Hep}$ mice to generate MUP-uPA-*Stard1*$^{\Delta Hep}$ mice and fed a HFHC diet (Fig. 3A). MUP-uPA-Stard1$^{\Delta Hep}$ mice exhibited profound depletion of *Stard1* expression in liver extracts with respect to MUP-uPA-*Stard1*$^{f/f}$ mice (Fig. 3B). Whereas feeding MUP-uPA-*Stard1*$^{f/f}$ mice with a HFHC diet for 26 weeks led to the development of liver tumours, the number and maximal area of these tumours in MUP-uPA-*Stard1*$^{\Delta Hep}$ mice were markedly reduced (Fig. 3C,D). This outcome was accompanied by a decrease in serum Afp levels (Fig. 3E) and lower expression of genes involved in fibrosis (*Col1a1* and *Acta2*) and inflammation (*Il6* and *Il1b*), and an attenuation in the levels of tumour markers (*Afp*, *Cd44* and *Ly6d*) (Fig. 3F–H). Interestingly, ablation of Stard1 did not affect the expression of ER stress markers in MUP-uPA-*Stard1*$^{\Delta Hep}$ mice (Fig. 3I,J), indicating that the inhibitory effect of *Stard1* deletion in this model of NASH-driven HCC was not linked to the prevention of ER stress.

In addition to this spontaneous NASH-driven HCC model, *Stard1*$^{\Delta Hep}$ mice were treated with DEN and then fed a HFHC diet for 24 weeks. Similar to the MUP-uPA model, DEN-treated *Stard1*$^{\Delta Hep}$ mice were relatively resistant to HFHC-mediated HCC development, exhibiting decreased tumour multiplicity and maximal area (Fig. 4A,B) and a decrease in the serum Afp levels (Fig. 4C). Tumours from *Stard1*$^{\Delta Hep}$ mice exhibited decreased Yap and Afp expression (Fig. 4D,E) and lower mRNA levels of tumour markers without a change in inflammation-related genes (Fig. 4F,G). This outcome was accompanied by

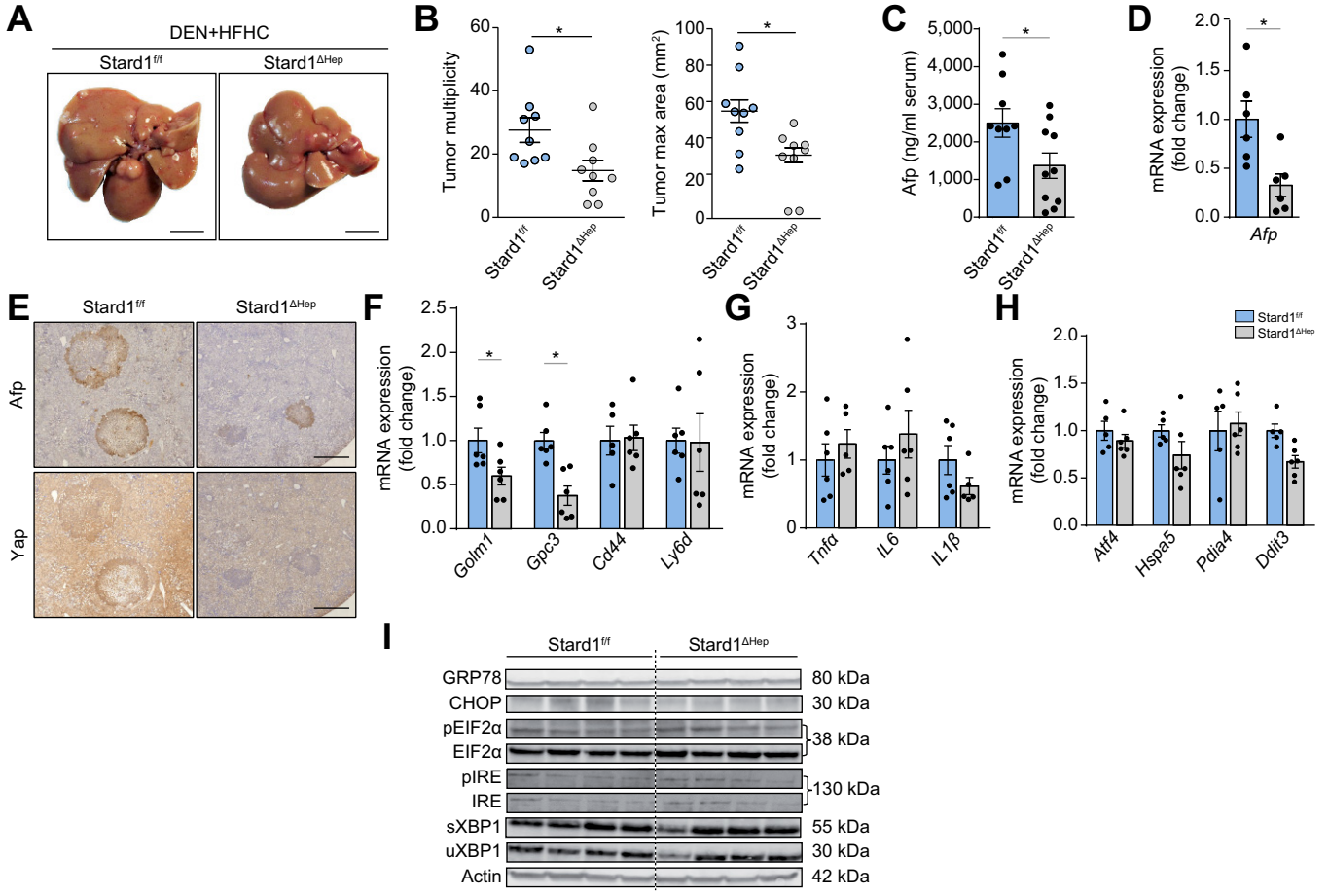

Fig. 4. *Stard1*$^{\Delta Hep}$ mice are less sensitive to DEN+HFHC-induced HCC. (A,B) Macroscopic images of livers from *Stard1*$^{f/f}$ (n = 9) and *Stard1*$^{\Delta Hep}$ mice (n = 9) treated with DEN and fed a HFHC diet for 24 weeks, with quantification of tumour multiplicity and maximal area. (C,D) Serum and mRNA expression levels of Afp from *Stard1*$^{f/f}$ (n = 9) and *Stard1*$^{\Delta Hep}$ mice (n = 9) treated with DEN and fed a HFHC diet. (E) Immunohistochemical expression of Afp and Yap of consecutive liver sections from *Stard1*$^{f/f}$ and *Stard1*$^{\Delta Hep}$ mice. (F,G) mRNA levels of tumour markers and inflammation genes of whole-liver tissue from *Stard1*$^{f/f}$ and *Stard1*$^{\Delta Hep}$ mice. (H) mRNA levels of ER stress markers of whole-liver tissue from *Stard1*$^{f/f}$ (n = 6) and *Stard1*$^{\Delta Hep}$ mice (n = 6). (I) Western blot of ER stress markers as in (H). All values are mean ± SEM. *p <0.05 with respect to MUP-uPA-*Stard1*$^{f/f}$ or *Stard1*$^{f/f}$ mice on a Student's t test. DEN, diethylnitrosamine; ER, endoplasmic reticulum; HCC, hepatocellular carcinoma; HFHC, high fat, high cholesterol; Stard1, steroidogenic acute regulatory protein 1.

unchanged expression of ER stress markers in DEN+HFHC-treated *Stard1*$^{\Delta Hep}$ mice (Fig. 4H,I). Thus, these findings support a crucial role of STARD1 in NASH-driven HCC independently of ER stress.

STARD1 overexpression exacerbates DEN+HFHC diet-driven HCC

To further investigate the contribution of STARD1 in NASH-driven HCC, *Stard1* was overexpressed in DEN+HFHC WT mice by injection with adenovirus bearing the cDNA of *Stard1* (AD-Stard1) 5 weeks before sacrifice (Fig. 5A), which resulted in a 15-fold increase in liver *Stard1* expression (mRNA and protein levels) compared with control mice injected with an empty control vector (AD-control) (Fig. 5A–C). This outcome potentiated DEN+HFHC-mediated liver tumour multiplicity, although the maximal area of tumours did not significantly change (Fig. 5D,E). The extent of expression of the HCC markers Afp and Yap in tumours was greater in the AD-Stard1 group (Fig. 5F). Consistent with these findings, expression of tumour markers (*Afp, Yap, Golm1* or *Krt19*) increased upon *Stard1* overexpression (Fig. 5G) and this outcome was accompanied by enhanced expression of inflammatory-related and hypoxia-regulated genes (Fig. 5H,I). In addition, liver oxidative stress, as measured by dihydroethidium staining of liver sections from DEN+HFHC mice overexpressing *Stard1*, was significantly higher than that measured in the AD-control group (Fig. 5J). Moreover, overexpression of Stard1 in subcutaneous tumours induced by TICs in immunodeficient mice resulted in the induction of genes involved in pluripotency and stemness (Fig. 5K), which paralleled the increase in tumour growth compared with TICs expressing a GFP control vector (Fig. 5L). The tumour-promoting effect of STARD1 required dietary cholesterol feeding (HC) (Fig. 5M), as indicated by the findings that *Stard1* overexpression in DEN+regular diet-fed mice or mice fed a HC diet alone for 24 weeks did not lead to HCC development (Fig. 5N,O). Overall, these findings indicate that STARD1 and dietary cholesterol synergise to promote HCC development.

STARD1 regulates the profile of hepatic BAs in NASH-driven HCC

Given that BAs have been linked to NASH progression and HCC development,[14,17–19] the study next addressed whether STARD1

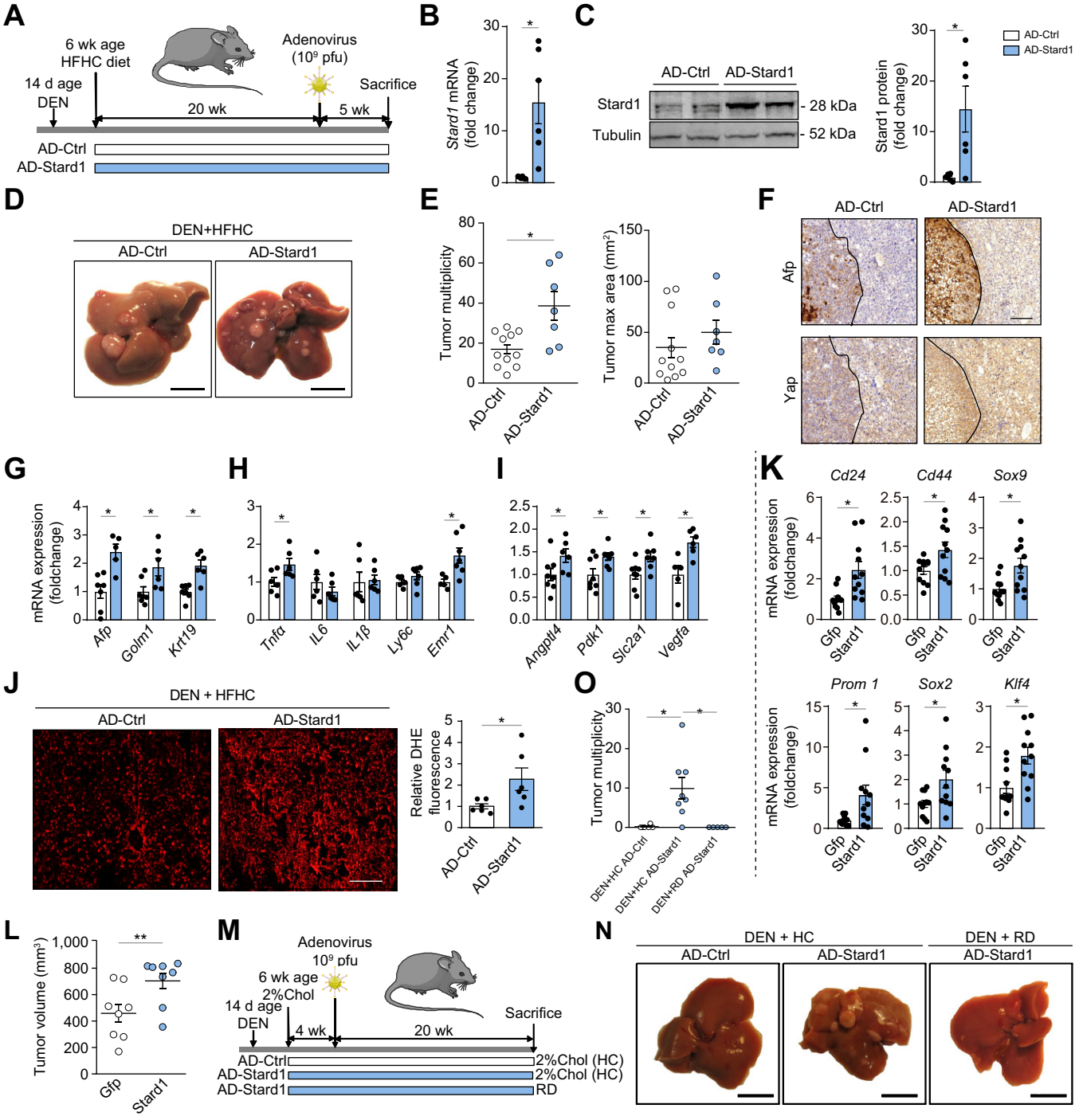

Fig. 5. Stard1 overexpression increases DEN+HFHC-driven HCC. (A) Schematic illustration of the experimental design used to overexpress *Stard1* in wild-type mice 5 months after DEN+HFHC treatment. (B) Adenoviral-induced overexpression of mouse *Stard1* in liver of mice determined by qPCR. n = 6 for each group. (C) Quantification of *Stard1* overexpression by immunoblot densitometry and representative image of a western blot for *Stard1*. n = 6 for each group. (D,E) Representative images of livers and quantification of macroscopic liver tumour multiplicity and maximum size in animals after 5 weeks of recombinant adenovirus injection; n = 11 for AD-Ctrl and n = 7 for AD-Stard1. (F) Immunohistochemistry of consecutive sections showing the same tumour (T, delimited by a dotted line) and parenchyma stained for Afp or Yap. Scale bar: 500 μm. (G–I) qPCR quantification of mRNA of HCC markers, fibrogenesis, inflammation and *Hif1a* target genes; n = 6 per group. (J) ROS production measured and quantified in cryosections of liver tissue stained with DHE (n = 6). (K) mRNA levels of stemness genes measured in subcutaneous tumours induced by TICs with or without *Stard1* overexpression. Values are mean ± SEM relative to GFP-expressing tumours (n = 12). **p* <0.05 with respect to matched GFP-expressing tumours on paired Student's *t* test. (L) Subcutaneous tumour volume in nude mice induced by TICs transfected with control GFP or Stard1. Values are mean ± SEM relative to GFP-expressing tumours (n = 8). **p* <0.05 with respect to matched GFP-expressing tumours on paired Student's *t* test. (M) Schematic experimental design for adenoviral-mediated *Stard1* overexpression (AD-Star) in DEN-treated wild-type mice followed by feeding a regular diet (RD) (n = 5) or a diet enriched in cholesterol (2%, HC) (n = 8) or AD-Ctrl on a HC diet (n = 6). (N,O) Macroscopic images of livers from DEN-treated mice and quantification of tumour multiplicity. All values are mean ± SEM. **p* <0.05 with respect to Ad-Ctrl on a Student's *t* test. DEN, diethylnitrosamine; DHE, dihydroethidium; HCC, hepatocellular carcinoma; HFD, high-fat diet; HC, high cholesterol; HFHC, high fat, high cholesterol; qPCR, quantitative PCR; RD, regular diet; ROS, reactive oxygen species; Stard1, steroidogenic acute regulatory protein 1; TIC, tumour-initiating stem-like cell.

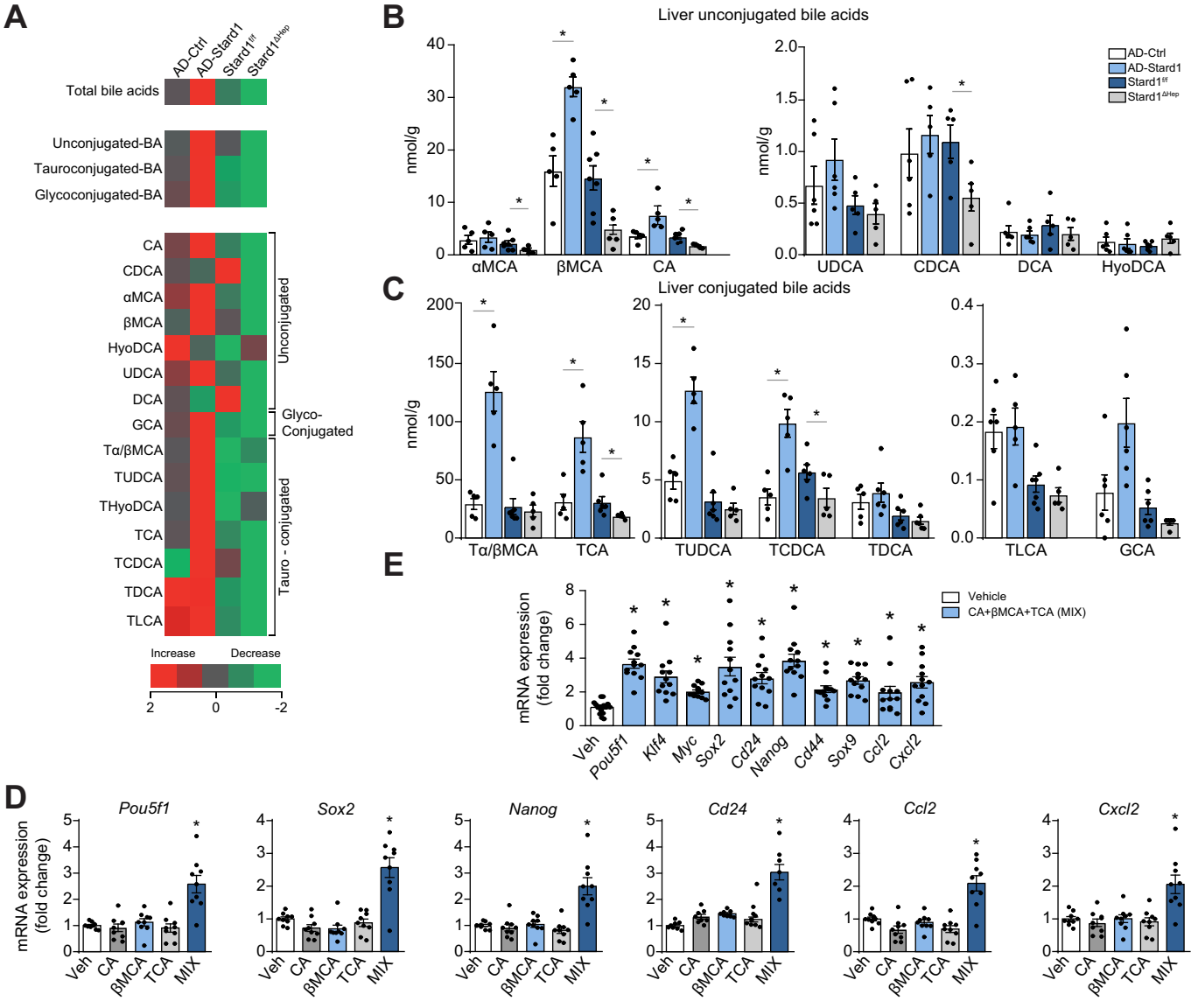

Fig. 6. Molecular species of BAs in NASH-HCC models and their impact on the expression of genes involved in self-renewal, stemness and inflammation. (A) Heatmap of individual species of BAs measured in livers from AD-*Stard1* mice and *Stard1*$^{\Delta Hep}$ mice following DEN treatment and HFHC feeding, showing an increase (red) or a reduction (green) with respect to the mean of AD-control and *Stard1*$^{f/f}$ mice. Values are Log2 of the fold change. (B) Quantification of the unconjugated BAs in liver tissue from each group of animals. (n = 5 for AD-Ctrl/AD-Stard1 and n = 6 for *Stard1*$^{f/f}$ and *Stard*$^{\Delta Hep}$ mice. (C) Quantification of tauroconjugated BAs in liver tissue from each group of animals. (D) mRNA levels of genes involved in self-renewal, stemness and inflammation in TICs following incubation with CA (50 μM), βMCA (50 μM) and TCA (200 μM) for 48 h. Values are mean ± SEM. n = 3 independent experiments performed in triplicate. (E) Effect of the combination of CA, βMCA and TCA in PMH for 24 h on the mRNA levels of genes involved in self-renewal, stemness and inflammation. Values are mean ± SEM. n = 3 independent experiments performed in quadruplicates. βMCA, β-muricholic acid; BA, bile acid; CA, cholic acid; DEN, diethylnitrosamine; HCC, hepatocellular carcinoma; HFHC, high fat, high cholesterol; NASH, non-alcoholic steatohepatitis; Stard1, steroidogenic acute regulatory protein 1; TCA, taurocholic acid.

regulates the profile of hepatic BAs in NASH-driven HCC. Mass spectrometry analyses were performed of the hepatic molecular species of BAs in WT mice with *Stard1* overexpression (AD-Stard1) and in *Stard1*$^{\Delta Hep}$ mice. The total BA content in liver increased in AD-Stard1 mice with respect to AD-Ctrl mice (Fig. 6A). These quantitative changes reflected the increase in unconjugated BAs, such as βMCA and CA and their tauroconjugated derivatives Tα/βMCA and TCA in AD-Stard1 mice, the levels of which were 1 order of magnitude higher than those of tauroursodeoxycholic acid (TUDCA) and taurochenodeoxycholic acid (TCDCA) (Fig. 6B,C). By contrast, the total liver BA burden in *Stard1*$^{\Delta Hep}$ mice significantly decreased compared with *Stard1*$^{f/f}$ mice, with lower levels of TCA, βMCA and CA (Fig. 6B,C). The amount of minor unconjugated Bas [*i.e.* ursodeoxycholic acid (UDCA), chenodeoxycholic acid (CDCA), dichloroacetic acid (DCA) and hyodeoxycholic acid (HyoDCA)] remained unchanged regardless of the status of *Stard1* expression (Fig. 6B). A similar decrease in the levels of βMCA, Tα/βMCs and TCA was observed in MUP-uPA-*Stard1*$^{\Delta Hep}$ mice with respect to MUP-uPA-*Stard*$^{f/f}$ mice (Fig. S5). The levels of the oxysterols 24S-hydroxycholesterol (24S-OH-Chol) and 27-hydroxycholesterol (27-OH-Chol), which are intermediates of BA synthesis in the acidic pathway,[30,31] did not change in

AD-Stard1 or *Stard1*$^{\Delta Hep}$ mice (Fig. S6A). Interestingly, the expression of *Cyp7a1*, *Cyp8b1*, *Cyp27a1* and *Cyp7b1* as well as *Cyp27a1* and *Cyp7a1* in AD-Stard1 or *Stard1*$^{\Delta Hep}$ mice remained unaltered (Fig. S6B–E). In addition, although the expression of FXR (*Nr1h4*) as well as that of *Nr0b2* and *Abcd11* decreased (50–60%) in AD-Stard1 mice overexpressing *Stard1*, the levels of *Nr1h4* and its target genes *Nr0b2*, *Abcb11* and *Abcb4* in DEN+HFHC *Stard1*$^{\Delta Hep}$ mice was similar to that in DEN+HFHC Stard1f/f mice (Fig. S6F), suggesting that the regulatory role of Stard1 in BA synthesis and HCC development is independent of FXR. These findings indicate that a significant proportion of hepatic BAs generated during HCC development are regulated by STARD1.

BAs induce the expression of genes involved in self-renewal, stemness and inflammation

To establish the link between STARD1-mediated regulation of BAs and HCC, the impact of the profile of BAs regulated by STARD1 was examined on the expression of transcription factors involved in self-renewal and pluripotency, which are of relevance for HCC pathogenesis.[39,51] TICs (CD133^{+}/CD49f^{+}) were previously characterised and isolated from murine HCC models and shown to exhibit oncogenic activity and tumourigenicity.[39,52,53] Treatment of TICs with a combination of CA, TCA and βMCA at a concentration mimicking the levels observed in AD-Stard1 mice overexpressing *Stard1* increased the expression of Yamanaka transcription factors *Sox2* and *Pouf51* as well as the stemness markers *Nanog* and *Cd24* and the inflammatory chemokines *Ccl2* and *Cxcl1* (Fig. 6D). Interestingly, the level of expression of pluripotency and early differentiation genes in mature liver was reported to be similar to those found in fetal liver and induced pluripotent stem cell (iPSC)-derived hepatocyte-like cells.[54] In line with previous findings,[14] the incubation of PMH with CA, TCA and βMCA significantly increased the expression of *Sox2*, *Myc*, *Klf4* and *Pouf51*, as well as the stemness-related and cancer stem cell markers *Cd24*, *Cd44*, *Sox9* and *Nanog*, and the inflammatory genes *Ccl2* and *Cxcl2* (Fig. 6E). Although CDCA and secondary BAs, DCA and lithocholic acid (LCA) were cytotoxic to TICs, lower concentrations (10 μM) of these BAs induced the expression of genes involved in self-renewal, stemness and inflammation (Fig. S6G).

Discussion

The NASH-driven HCC subset is a growing public health burden and is expected to increase worldwide because of its association with obesity and type 2 diabetes mellitus. Extending previous observations on the alterations of cholesterol homeostasis in human NASH,[33,34] we showed here an upregulation in the expression of STARD1 in patients with NASH-derived HCC. Importantly, increasing or decreasing the expression of *Stard1* in mice resulted in the stimulation or attenuation, respectively, of liver cancer, indicating that the induction of STARD1 in patients could be a cause of NASH-driven HCC. The physiological role of STARD1 in the liver is to provide cholesterol to the mitochondrial inner membrane for its biotransformation into BAs; however, the contribution of this pathway to NASH-driven HCC had not been previously explored. Here, we provide evidence that STARD1 expression determines the level and composition of hepatic BAs in models of NASH-driven HCC, and establish a link whereby STARD1 promotes HCC by stimulating the synthesis of BAs through the mitochondrial alternative pathway.

The metabolism of cholesterol within mitochondria begins by its hydroxylation at position 27 by CYP27A1, yielding 27-OH-chol, which then feeds BA synthesis via CYP7B1 to generate CDCA. STARD1 rather than CYP27A1 is the rate-limiting step in the alternative pathway of BA synthesis. As shown in primary hepatocytes or HepG2 cells, the overexpression of STARD1 resulted in a 5-fold increase in the rate of BA synthesis, whereas transfection with CYP27A1 upregulated BA synthesis by 2-fold.[55,56] In line with this notion, the impact of modulating STARD1 expression in NASH-driven HCC development parallels the generation of BA species, with an increased or decreased total BA pool in mice overexpressing *Stard1* or *Stard1*$^{\Delta Hep}$ mice, respectively, whereas the levels of oxysterols 24S-OH-chol and 27-OH-chol remained unaltered. Moreover, these effects of STARD1 expression on BA synthesis through the alternative pathway were not dependent on the status of *Cyp27a1*/*Cyp7b1* expression, which remained unchanged regardless of STARD1 levels, further establishing the crucial role of STARD1 in regulating cholesterol biotransformation into BAs. These findings imply that, although the classical pathway regulated by CYP7A1 is considered the predominant route of cholesterol-mediated BA synthesis in hepatocytes, the STARD1-dependent BA synthesis through the alternative pathway might take over the classical pathway in diseased states in which both cholesterol and STARD1 are induced, such as NASH-driven HCC. In line with this possibility, ER stress, a crucial player in NASH-HCC development, has been identified as a new mechanism that regulates BA synthesis by decreasing the expression of CYP7A1.[57] CA is the predominant BA synthesised through the classical pathway regulated by CYP7A1, which requires the action of CYP8B1 to add the 12α-hydroxylation characteristic of CA. By contrast, the other primary BA (*i.e.* CDCA) is predominantly synthesised through the alternative pathway via CYP27A1 and CYP7B1. Whereas in humans, CDCA is further metabolised by intestinal bacteria to LCA, CDCA in rodents is biotransformed by hepatocytes, through what can be considered a surrogate of the alternative pathway of BA synthesis, into the trihydroxylated BA αMCA in positions 3α, 6β and 7α and its 7β-epimer βMCA.[15,30–32] Accordingly, our data indicate that modulation of *Stard1* expression in mice by its overexpression or deletion in hepatocytes resulted in increased or curtailed levels of βMCA and its tauroconjugated form, TβMC, a potent FXR antagonist that relieves the FXR-mediated down-regulation of CYP7A1 but not of CYP27A1.[58,59] The lack of change in the expression of CYP7A1 in the NASH-driven HCC might reflect the counterbalance between the indirect stimulating effect of TβMCA via antagonism of FXR and the suppressing action of chronic ER stress.[57] Intriguingly, we show an unanticipated STARD1-dependent modulation of CA and its subsequent TCA generation in NASH-driven HCC. In line with this link, it was recently described that, in addition to the conversion of 7α-hydroxycholest-4-en-3-one to 7α, 12α-dihydroxycholest-4-en-3-one, CYP8B1 can also biotransform CDCA itself into CA.[60]

To address whether the tumour-promoter role of STARD1 in NASH-driven HCC is linked to the regulation of the alternative pathway of BAs synthesis, the study examined the impact of BAs (CA, βMCA and TCA) mimicking the profile regulated by STARD1 in the expression of self-renewal and stemness genes involved in HCC.[39,51] This profile of BAs induced the expression of genes involved in self-renewal, stemness and inflammation in TICs and PMH. Of interest, the findings in PMH were in line with previous reports indicating a similar level of expression of pluripotency

and early differentiation genes in mature liver versus fetal liver or iPSC-derived hepatocyte-like cells.[14,54] Moreover, the direct link between STARD1 and BA synthesis through the alternative pathway in HCC pathogenesis was consistent with the recognised role of BAs in promoting NASH progression and HCC development.[16–19] Feeding WT mice with a CA-enriched diet increased the hepatic BA pool and potentiated liver carcinogenesis.[14] Furthermore, the spontaneous development of HCC in *Fxr*$^{-/-}$ mice was shown to be reversed by decreasing BA levels by cholestyramine,[17,19] which is reminiscent of the outcome in *Stard1*$^{\Delta Hep}$ mice.

Characterisation of the molecular BA species directly regulated by STARD1 expression has been limited to mice. Whereas in human NASH-driven HCC samples, a correlation was observed between STARD1 expression and the increased total hepatic BA pool, full characterisation of the individual BAs generated would require an increased sample size to allow mass spectrometry analysis. In this regard, we undertook an initial approach to address the role of the secondary BAs DCA plus LCA, which, in addition to their cytotoxic effects in TICs, induced the expression of genes involved in self-renewal, stemness and inflammation. Another intriguing finding that requires further research is the role of TUDCA in STARD1-dependent HCC development. Although exogenous administration of TUDCA has been shown to protect against liver tumourigenesis because of its anti-ER stress effects,[7,8] the levels of TUDCA generated in AD-Stard1 mice were 1 order of magnitude lower than of tauro-muricholic acid and TCA.

Abbreviations

24S-OH-chol, 24S-hydroxycholesterol; 27-OH-chol, 27-hydroxycholesterol; βMCA, 7β-epimer β-muricholic acid; ALT, aminotransferase; BA, bile acids; CA, cholic acid; CDCA, chenodeoxycholic acid; DCA, dichloroacetic acid; DEN, diethylnitrosamine; ER, endoplasmic reticulum; EZE, ezetimibe; FXR, farnesoid X receptor; GST-PFO, GST-perfringolysin; HFD, high-fat diet; HFHC, high-fat high-cholesterol diet; HyoDCA, hyodeoxycholic acid; iPSC, induced pluripotent stem cell; NASH, non-alcoholic steatohepatitis; PBC, primary biliary cholangitis; PMH, primary mouse hepatocyte; STARD1, steroidogenic acute regulatory protein 1; TCA taurocholic acid; TCDCA, taurochenodeoxycholic acid; TG, triglyceride; TGR5, Takeda G-protein-coupled receptor 5; TIC, tumour-initiating stem-like cell; TNF, tumour necrosis factor; TUDCA, tauroursodeoxycholic acid; UDCA, ursodeoxycholic acid; uPA, urokinase plasminogen activator; WT, wild-type.

Financial support

We acknowledge support from grants PID2019-111669RB-100, SAF2017-85877R and SAF2015-73579-JIN from Plan Nacional de I+D funded by the Agencia Estatal de Investigación (AEI), the Fondo Europeo de Desarrollo Regional (FEDER) and CIBEREHD; the center grant P50AA011999 Southern California Research Center for ALPD and Cirrhosis funded by NIAAA / NIH; as well as support from AGAUR of the Generalitat de Catalunya SGR-2017-1112, European Cooperation in Science & Technology (COST) ACTION CA17112 Prospective European Drug-Induced Liver Injury Network, the 'ER stress-mitochondrial cholesterol axis in obesity-associated insulin resistance and comorbidities'-Ayudas FUNDACION BBVA and the Red Nacional 2018-102799-T de Enfermedades Metabólicas y Cáncer, and Project 201916/31 "Contribution of mitochondrial oxysterol and bile acid metabolism to liver carcinogenesis" 2019 by Fundació Marato TV3. We also acknowledge the support from the Fondo de Investigaciones Sanitarias, Instituto de Salud Carlos III, Spain (PI16/00598, co-funded by European Regional Development Fund / European Social Fund, 'Investing in your future') and Centro Internacional sobre el Envejecimiento (OLD-HEPAMARKER, 0348_CIE_6_E), Spain. We also acknowledge support from R01 CA2344128 and U01 AA022614 grants to M.K.

Conflicts of interest

The authors declare no conflicts of interest that pertain to this work.

Please refer to the accompanying ICMJE disclosure forms for further details.

Authors' contributions

Conceptualisation: C.G.-R., V.R. and J.C.F.-Ch. Methodology: L.C.R., M.J.M., J.J.G, L.B-R., A.C., F.C., J.C.G.-V., J.Fu. and J.Fe. Investigation: L.C.R., C.V., A.B., S.N., V.R., and C.G.-R. Formal analysis: L.C.R., M.J.M., J.J.G, C.G.-R., V.R and J.C.F.-Ch. Supervision and funds acquisition: C.G.-R, V.R. and J.C.F.-Ch. Writing: review & editing: C.G.-R, V.R., M.J.M., J.J.G., M.K, and J.C.F.-Ch.

Data availability statement

Data that support the study findings are available upon reasonable request from the corresponding authors (C.G.-R., V.R. and J.C.F.-Ch). Detailed information on experimental protocols may also be shared on reasonable request.

Acknowledgements

MUP-uPA transgenic mice were kindly provided by Eric P. Sandgren from the University of Wisconsin-Madison (Madison, WI, USA). We are grateful to Keigo Machida (University of Southern California, LA, USA) for the generous gift of TICs. We are indebted to the Biobank core facility of the Instituto de Investigaciones Biomédicas August Pi i Sunyer (IDIBAPS) for technical help. This work was developed at the Centre Esther Koplowitz, Barcelona, Spain. We also thank Fabián Arenas for help with graphic design.

Supplementary data

Supplementary data to this article can be found online at https://doi.org/10.1016/j.jhep.2021.01.028.

References

Author names in bold designate shared co-first authorship

[1] Bianchini F, Kaaks R, Vainio H. Overweight, obesity, and cancer risk. Lancet Oncol 2002;3:565–574.
[2] Calle EE, Rodriguez C, Walker-Thurmond K, Thun MJ. Overweight, obesity, and mortality from cancer in a prospectively studied cohort of U.S. adults. N Engl J Med 2003;348:1625–1638.
[3] Forner A, Reig M, Bruix J. Hepatocellular carcinoma. Lancet 2018;391:1301–1314.
[4] Bruix J, Reig M, Sherman M. Evidence-based diagnosis, staging, and treatment of patients with hepatocellular carcinoma. Gastroenterology 2016;150:835–853.
[5] Villanueva A, Hernandez-Gea V, Llovet JM. Medical therapies for hepatocellular carcinoma: a critical view of the evidence. Nat Rev Gastroenterol Hepatol 2013;10:34–42.

[6] Marin JJG, Herraez E, Lozano E, Macias RIR, Briz O. Models for understanding resistance to chemotherapy in liver cancer. Cancers (Basel) 2019;11:1677.
[7] Park EJ, Lee JH, Yu GY, He G, Ali SR, Holzer RG, et al. Dietary and genetic obesity promote liver inflammation and tumorigenesis by enhancing IL-6 and TNF expression. Cell 2010;140:197–208.
[8] Nakagawa H, Umemura A, Taniguchi K, Font-Burgada J, Dhar D, Ogata H, et al. ER stress cooperates with hypernutrition to trigger TNF-dependent spontaneous HCC development. Cancer Cell 2014;26:331–343.
[9] Febbraio MA, Reibe S, Shalapour S, Ooi GJ, Watt MJ, Karin M. Preclinical models for studying NASH-driven HCC: how useful are they? Cell Metab 2019;29:18–26.
[10] Che L, Chi W, Qiao Y, Zhang J, Song X, Liu Y, et al. Cholesterol biosynthesis supports the growth of hepatocarcinoma lesions depleted of fatty acid synthase in mice and humans. Gut 2020;69:177–186.
[11] Liang JQ, Teoh N, Xu L, Pok S, Li X, Chu ESH, et al. Dietary cholesterol promotes steatohepatitis related hepatocellular carcinoma through dysregulated metabolism and calcium signaling. Nat Commun 2018;9:4490.
[12] Bakiri L, Hamacher R, Grana O, Guio-Carrion A, Campos-Olivas R, Martinez L, et al. Liver carcinogenesis by FOS-dependent inflammation and cholesterol dysregulation. J Exp Med 2017;214:1387–1409.
[13] Liu D, Wong CC, Fu L, Chen H, Zhao L, Li C, et al. Squalene epoxidase drives NAFLD-induced hepatocellular carcinoma and is a pharmaceutical target. Sci Transl Med 2018;10:eaap9840.
[14] Sun L, Beggs K, Borude P, Edwards G, Bhushan B, Walesky C, et al. Bile acids promote diethylnitrosamine-induced hepatocellular carcinoma via increased inflammatory signaling. Am J Physiol Gastrointest Liver Physiol 2016;311:G91–G104.
[15] Gadaleta RM, van Mil SW, Oldenburg B, Siersema PD, Klomp LW, van Erpecum KJ. Bile acids and their nuclear receptor FXR: relevance for hepatobiliary and gastrointestinal disease. Biochim Biophys Acta 2010;1801:683–692.
[16] Puri P, Daita K, Joyce A, Mirshahi F, Santhekadur PK, Cazanave S, et al. The presence and severity of nonalcoholic steatohepatitis is associated with specific changes in circulating bile acids. Hepatology 2018;67:534–548.
[17] Kim I, Morimura K, Shah Y, Yang Q, Ward JM, Gonzalez FJ. Spontaneous hepatocarcinogenesis in farnesoid X receptor-null mice. Carcinogenesis 2007;28:940–946.
[18] Knisely AS, Strautnieks SS, Meier Y, Stieger B, Byrne JA, Portmann BC, et al. Hepatocellular carcinoma in ten children under five years of age with bile salt export pump deficiency. Hepatology 2006;44:478–486.
[19] Yang F, Huang X, Yi T, Yen Y, Moore DD, Huang W. Spontaneous development of liver tumors in the absence of the bile acid receptor farnesoid X receptor. Cancer Res 2007;67:863–867.
[20] **Mari M**, **Caballero F**, Colell A, Morales A, Caballeria J, Fernandez A, et al. Mitochondrial free cholesterol loading sensitizes to TNF- and Fas-mediated steatohepatitis. Cell Metab 2006;4:185–198.
[21] **Solsona-Vilarrasa E**, **Fucho R**, Torres S, Nunez S, Nuno-Lambarri N, Enrich C, et al. Cholesterol enrichment in liver mitochondria impairs oxidative phosphorylation and disrupts the assembly of respiratory supercomplexes. Redox Biol 2019;24:101214.
[22] Montero J, Morales A, Llacuna L, Lluis JM, Terrones O, Basanez G, et al. Mitochondrial cholesterol contributes to chemotherapy resistance in hepatocellular carcinoma. Cancer Res 2008;68:5246–5256.
[23] Lucken-Ardjomande S, Montessuit S, Martinou JC. Bax activation and stress-induced apoptosis delayed by the accumulation of cholesterol in mitochondrial membranes. Cell Death Differ 2008;15:484–493.
[24] Christenson E, Merlin S, Saito M, Schlesinger P. Cholesterol effects on BAX pore activation. J Mol Biol 2008;381:1168–1183.
[25] Smith B, Land H. Anticancer activity of the cholesterol exporter ABCA1 gene. Cell Rep 2012;2:580–590.
[26] Ribas V, Garcia-Ruiz C, Fernandez-Checa JC. Mitochondria, cholesterol and cancer cell metabolism. Clin Transl Med 2016;5:22.
[27] Alpy F, Tomasetto C. START ships lipids across interorganelle space. Biochimie 2014;96:85–95.
[28] Clark BJ. The mammalian START domain protein family in lipid transport in health and disease. J Endocrinol 2012;212:257–275.
[29] Elustondo P, Martin LA, Karten B. Mitochondrial cholesterol import. Biochim Biophys Acta Mol Cell Biol Lipids 2017;1862:90–101.
[30] Pandak WM, Kakiyama G. The acidic pathway of bile acid synthesis: not just an alternative pathway. Liver Res 2019;3:88–98.
[31] Kakiyama G, Marques D, Takei H, Nittono H, Erickson S, Fuchs M, et al. Mitochondrial oxysterol biosynthetic pathway gives evidence for CYP7B1 as controller of regulatory oxysterols. J Steroid Biochem Mol Biol 2019;189:36–47.
[32] Vaz FM, Ferdinandusse S. Bile acid analysis in human disorders of bile acid biosynthesis. Mol Aspects Med 2017;56:10–24.
[33] Caballero F, Fernandez A, De Lacy AM, Fernandez-Checa JC, Caballeria J, Garcia-Ruiz C. Enhanced free cholesterol, SREBP-2 and StAR expression in human NASH. J Hepatol 2009;50:789–796.
[34] Min HK, Kapoor A, Fuchs M, Mirshahi F, Zhou H, Maher J, et al. Increased hepatic synthesis and dysregulation of cholesterol metabolism is associated with the severity of nonalcoholic fatty liver disease. Cell Metab 2012;15:665–674.
[35] Mazzaferro V, Regalia E, Doci R, Andreola S, Pulvirenti A, Bozzetti F, et al. Liver transplantation for the treatment of small hepatocellular carcinomas in patients with cirrhosis. N Engl J Med 1996;334:693–699.
[36] **Torres S**, **Baulies A**, Insausti-Urkia N, Alarcon-Vila C, Fucho R, Solsona-Vilarrasa E, et al. Endoplasmic reticulum stress-induced upregulation of STARD1 promotes acetaminophen-induced acute liver failure. Gastroenterology 2019;157:552–568.
[37] Weglarz TC, Degen JL, Sandgren EP. Hepatocyte transplantation into diseased mouse liver. Kinetics of parenchymal repopulation and identification of the proliferative capacity of tetraploid and octaploid hepatocytes. Am J Pathol 2000;157:1963–1974.
[38] **Baulies A**, **Montero J**, Matias N, Insausti N, Terrones O, Basanez G, et al. The 2-oxoglutarate carrier promotes liver cancer by sustaining mitochondrial GSH despite cholesterol loading. Redox Biol 2018;14:164–177.
[39] Chen CL, Tsukamoto H, Liu JC, Kashiwabara C, Feldman D, Sher L, et al. Reciprocal regulation by TLR4 and TGF-beta in tumor-initiating stem-like cells. J Clin Invest 2013;123:2832–2849.
[40] Arenas F, Castro F, Nunez S, Gay G, Garcia-Ruiz C, Fernandez-Checa JC. STARD1 and NPC1 expression as pathological markers associated with astrogliosis in post-mortem brains from patients with Alzheimer's disease and Down syndrome. Aging 2020;12:571–592.
[41] Kim JY, Garcia-Carbonell R, Yamachika S, Zhao P, Dhar D, Loomba R, et al. ER stress drives lipogenesis and steatohepatitis via caspase-2 activation of S1P. Cell 2018;175:133–145.
[42] Yang Z, Qin W, Chen Y, Yuan B, Song X, Wang B, et al. Cholesterol inhibits hepatocellular carcinoma invasion and metastasis by promoting CD44 localization in lipid rafts. Cancer Lett 2018;429:66–77.
[43] Zhao Z, Zhong L, He K, Qiu C, Li Z, Zhao L, et al. Cholesterol attenuated the progression of DEN-induced hepatocellular carcinoma via inhibiting SCAP mediated fatty acid de novo synthesis. Biochem Biophys Res Commun 2019;509:855–861.
[44] Lee YL, Li WC, Tsai TH, Chiang HY, Ting CT. Body mass index and cholesterol level predict surgical outcome in patients with hepatocellular carcinoma in Taiwan - a cohort study. Oncotarget 2016;7:22948–22959.
[45] Carr BI, Giannelli G, Guerra V, Giannini EG, Farinati F, Rapaccini GL, et al. Plasma cholesterol and lipoprotein levels in relation to tumor aggressiveness and survival in HCC patients. Int J Biol Markers 2018;33:423–431.
[46] Qin WH, Yang ZS, Li M, Chen Y, Zhao XF, Qin YY, et al. High serum levels of cholesterol increase anti-tumor functions of nature killer cells and reduce growth of liver tumors in mice. Gastroenterology 2020;158:1713–1727.
[47] Jang JE, Park HS, Yoo HJ, Baek IJ, Yoon JE, Ko MS, et al. Protective role of endogenous plasmalogens against hepatic steatosis and steatohepatitis in mice. Hepatology 2017;66:416–431.
[48] Farrell G, Schattenberg JM, Leclercq I, Yeh MM, Goldin R, Teoh N, et al. Mouse models of nonalcoholic steatohepatitis: toward optimization of their relevance to human nonalcoholic steatohepatitis. Hepatology 2019;69:2241–2257.
[49] Loomba R, Sirlin CB, Ang B, Bettencourt R, Jain R, Salotti J, et al. Ezetimibe for the treatment of nonalcoholic steatohepatitis: assessment by novel magnetic resonance imaging and magnetic resonance elastography in a randomized trial (MOZART trial). Hepatology 2015;61:1239–1250.
[50] Miura K, Ohnishi H, Morimoto N, Minami S, Ishioka M, Watanabe S, et al. Ezetimibe suppresses development of liver tumors by inhibiting angiogenesis in mice fed a high-fat diet. Cancer Sci 2019;110:771–783.
[51] Lobo NA, Shimono Y, Qian D, Clarke MF. The biology of cancer stem cells. Annu Rev Cell Dev Biol 2007;23:675–699.
[52] Rountree CB, Ding W, He L, Stiles B. Expansion of CD133-expressing liver cancer stem cells in liver-specific phosphatase and tensin homolog deleted on chromosome 10-deleted mice. Stem Cells 2009;27:290–299.
[53] Ding W, Mouzaki M, You H, Laird JC, Mato J, Lu SC, et al. CD133+ liver cancer stem cells from methionine adenosyl transferase 1A-deficient

mice demonstrate resistance to transforming growth factor (TGF)-beta-induced apoptosis. Hepatology 2009;49:1277–1286.
[54] Zabulica M, Srinivasan RC, Vosough M, Hammarstedt C, Wu T, Gramignoli R, et al. Guide to the assessment of mature liver gene expression in stem cell-derived hepatocytes. Stem Cells Dev 2019;28:907–919.
[55] Pandak WM, Ren S, Marques D, Hall E, Redford K, Mallonee D, et al. Transport of cholesterol into mitochondria is rate-limiting for bile acid synthesis via the alternative pathway in primary rat hepatocytes. J Biol Chem 2002;277:48158–48164.
[56] Ren S, Hylemon PB, Marques D, Gurley E, Bodhan P, Hall E, et al. Overexpression of cholesterol transporter StAR increases in vivo rates of bile acid synthesis in the rat and mouse. Hepatology 2004;40:910–917.
[57] Henkel AS, LeCuyer B, Olivares S, Green RM. Endoplasmic reticulum stress regulates hepatic bile acid metabolism in mice. Cell Mol Gastroenterol Hepatol 2017;3:261–271.
[58] Sayin SI, Wahlstrom A, Felin J, Jantti S, Marschall HU, Bamberg K, et al. Gut microbiota regulates bile acid metabolism by reducing the levels of tauro-beta-muricholic acid, a naturally occurring FXR antagonist. Cell Metab 2013;17:225–235.
[59] Worthmann A, John C, Ruhlemann MC, Baguhl M, Heinsen FA, Schaltenberg N, et al. Cold-induced conversion of cholesterol to bile acids in mice shapes the gut microbiome and promotes adaptive thermogenesis. Nat Med 2017;23:839–849.
[60] Fan L, Joseph JF, Durairaj P, Parr MK, Bureik M. Conversion of chenodeoxycholic acid to cholic acid by human CYP8B1. Biol Chem 2019;400:625–628.